NeuroImage: Clinical 11 (2016) 378–387

Contents lists available at ScienceDirect

NeuroImage: Clinical

journal homepage: www.elsevier.com/locate/ynicl

Quantitative comparisons on hand motor functional areas determined by resting state and task BOLD fMRI and anatomical MRI for pre-surgical planning of patients with brain tumors

Bob L. Hou[a,*], Sanjay Bhatia[b], Jeffrey S. Carpenter[a]

[a] Department of Radiology, WVU, Morgantown, WV 26506, USA
[b] Department of Neurosurgery, WVU, Morgantown, WV 26506, USA

ARTICLE INFO

Article history:
Received 8 December 2015
Received in revised form 17 February 2016
Accepted 1 March 2016
Available online 2 March 2016

Keywords:
Localizing hand motor area
Task- and resting state-functional MR images
Anatomical T1wighted images
Brain tumor

ABSTRACT

For pre-surgical planning we present quantitative comparison of the location of the hand motor functional area determined by right hand finger tapping BOLD fMRI, resting state BOLD fMRI, and anatomically using high resolution T1 weighted images. Data were obtained on 10 healthy subjects and 25 patients with left sided brain tumors. Our results show that there are important differences in the locations (i.e., >20 mm) of the determined hand motor voxels by these three MR imaging methods. This can have significant effect on the pre-surgical planning of these patients depending on the modality used. In 13 of the 25 cases (i.e., 52%) the distances between the task-determined and the rs-fMRI determined hand areas were more than 20 mm; in 13 of 25 cases (i.e., 52%) the distances between the task-determined and anatomically determined hand areas were >20 mm; and in 16 of 25 cases (i.e., 64%) the distances between the rs-fMRI determined and anatomically determined hand areas were more than 20 mm. In just three cases, the distances determined by all three modalities were within 20 mm of each other. The differences in the location or fingerprint of the hand motor areas, as determined by these three MR methods result from the different underlying mechanisms of these three modalities and possibly the effects of tumors on these modalities.

1. Introduction

Location of "fingerprints" of the voxels for hand function in the primary sensory-motor cortex is an important part of the pre-operative evaluation of a patient when surgery near this area is being contemplated. The pre-operative localization of the hand area in the cortex of the hemisphere with brain lesions and its relation to the pathology allows targeted craniotomies and safer surgery for the patient. Confirmation by appropriate cortical stimulation, and in combination with diffusion tensor imaging (DTI), subcortical motor tract identification allows removal of tumors in close proximity to the motor cortex and tracts while minimizing the risk of contralateral weakness or paralysis (Emerson and Turner, 1993). Even though the hand functional areas of the motor cortex can often be localized by anatomical landmarks alone (Yousry et al., 1997), functional localization based on anatomy can often be unreliable (Alkhadi et al., 2000; Carpentier et al., 2001; Duffau, 2001; Mesulam, 2000; Rutten and Ramsey, 2010) for a patient with brain disease. The anatomy may be distorted, shifted, and unclear because of the lesion itself or the edema surrounding the lesion.

Among all the pre-operative noninvasive techniques to localize the sensory and motor cortex including a task driven functional MRI (fMRI), PET, magnetoencephalography (MEG), and transcranial magnetic stimulation (TMS), the task driven fMRI has become a de facto standard. Many studies have validated the results obtained by the fMRI with the 'gold standard' of intra-operative electrical stimulation (Majos et al., 2005; Fandino et al., 1999; Lehericy et al., 2000; Bizzi et al., 2008; Roessler et al., 2005). One of fMRI modalities measures changes in the ratio of oxygenated to deoxygenated hemoglobin in capillary beds because of their different magnetic properties. This technique called Blood Oxygen Level Dependent (BOLD) fMRI allows mapping of cortical areas based on task activated local field potentials and their coupling with the local vasculature causing changes in the levels of oxygenated hemoglobin due to the changes in the cerebral metabolic rate of oxygen consumption (CMRO2), cerebral blood flow (CBF) and cerebral blood volume (CBV) (Buxton et al., 2004). Because this technique requires patient participation, an optimal task performance may not occur in several groups of patients including young children or the elderly or those with paresis or cognitive deficits, either inherent or as a consequence of medications, drugs or anesthesia.

A recent advance in BOLD signal imaging is the resting state fMRI (rs-fMRI), which can obviate many of these difficulties. rs-fMRI is based on a hypothesis of spontaneously occurring low frequency fluctuations in

* Corresponding author at: 1 Medical Center Dr., PO Box 9235, Department of Radiology, WVU, Morgantown, WV 26506, USA.
E-mail address: bhou@hsc.wvu.edu (B.L. Hou).

http://dx.doi.org/10.1016/j.nicl.2016.03.003

the BOLD signal in brain cortices in the resting state, and these fluctuations being synchronous in several functionally connected areas (Biswal et al., 1995; Lowe et al., 2001; Cordes et al., 2001; Foz and Raichle, 2007; Zou et al., 2010; Raichle et al., 2001). rs-fMRI has become a popular tool to investigate brain functional connectivity (FC) (Fiecas et al., 2013; Biswal et al., 2010; Uddin et al., 2009; Long et al., 2008; Deshpande et al., 2011) after the studies of Biswal (Biswal et al., 1995) and Raichle (Raichle et al., 2001). A resting state network connecting the sensory and motor cortex has been shown in healthy subjects and patients (Xiong et al., 1999; Cordes et al., 2000; De Luca et al., 2005). Because the locations of the hand area in the primary sensory-motor cortex for healthy subjects and patients, determined by a rs-fMRI and a motor task BOLD fMRI methods, happen to be close (especially the cortex was determined by a group analysis), recent studies have attempted to use the resting state network (i.e., the sensory and motor network) as a localizing tool to preoperatively identify the hand area in the primary sensory-motor cortex in patients with brain tumors (Kokkonen et al., 2009; Zhang et al., 2009; Liu et al., 2009; Otten et al., 2009; Mannfolk et al., 2011) for maximizing resection of the tumor while minimizing damage to the eloquent cortex.

However, these attempts need to be verified by a quantitative study, i.e., is the "fingerprint" or the location of the hand area in the sensory and motor network determined by resting state BOLD signal the same as the one determined from a motor task BOLD signal and how do these relate to the anatomical localization of the hand area in the motor cortex? We hypothesized that the location of brain connected areas (i.e., the voxels) for hand motor function determined from rs-BOLD fMRI data is different from both the locations of the hand function areas determined by a finger tapping task BOLD fMRI data and anatomical MR images. We located fingerprints of the hand functional areas generated from the right hand finger tapping BOLD fMRI, rs-BOLD fMRI data and high resolution T1 weighted images in 10 healthy subjects and 25 patients with left hemispheric brain tumors, without previous surgery, and measured the differences between the locations of the hand functional areas determined from these two BOLD signals and the anatomical landmarks. We also discuss the mechanisms that may be responsible for our findings. To our knowledge, this paper is the first to quantitatively evaluate the differences in the locations or fingerprints of the hand motor areas determined by three MRI modalities in the patients with the brain tumors in the left hemispheres.

2. Patients and healthy subjects and methods

2.1. Patients and healthy subjects

In this study, 25 patients (41.6 ± 17.6 years) with a brain tumor in the left temporal and or frontal lobe(s) and 10 healthy subjects (35.2 ± 14.8 years) were included. The local authority approved the IRBs, in which the resting state BOLD fMRI was included. The relevant characteristics of these patients and healthy subjects are listed in Tables 1 and 2.

Table 1
Patients with brain tumors.

No.	Sex/age	Tumor type	Tumor location
1	F/33	Astrocytoma (II)	Left frontal and temporal
2	M/49	Oligodendroglioma (II)	Left temporal
3	F/64	Astrocytoma (II)	Left frontal and temporal
4	F/23	Oligodendroglioma (II)	Left temporal
5	F/51	Astrocytoma (III)	Left temporal
6	M/16	GBM (IV)	Left temporal
7	M/40	Diffuse astrocytoma (II)	Left temporal
8	M/36	Oligodendroglioma (II)	Left temporal
9	F/79	Astrocytoma (II)	Left temporal
10	F/43	Oligodendroglioma (III)	Left temporal
11	F/29	Astrocytoma (III)	Left temporal
10	F/47	Meningiomas	Left temporal
13	M/21	Gliosarcoma (IV)	Left frontal and temporal
14	F/44	Oligodendroglioma (II)	Left frontal and temporal
15	M/18	Astrocytoma (III)	Left temporal
16	F/18	Astrocytoma (II)	Left temporal
17	M/56	Astrocytoma (III)	Left temporal
18	F/17	Astrocytoma (II)	Left temporal
19	M/60	Oligodendroglioma (II)	Left temporal
20	M/29	Astrocytoma (II)	Left temporal
21	M/58	Astrocytoma (III)	Left temporal
22	F/37	Gliosarcoma (IV)	Left temporal
23	F/60	Oligodendroglioma (II)	Left temporal
24	M/44	Astrocytoma (II)	Left temporal
25	M/68	Astrocytoma (II)	Left temporal

2.2. Data acquisition

The anatomical imaging and task fMRI and rs-fMRI scans for each subject were performed using a 3.0 Tesla scanner with a 12-channel head matrix coil. A fast spin echo pulse sequence (TR/TE: 1900 ms/2.99 ms, slice thickness: 0.9 mm and number of axial slices:176) was applied for performing a T1-weighted high spatial resolution imaging. The rs-fMRI and fMRI scans were performed by using a multi slice 2D EPI (TR/TE: 3000 ms/30 ms, field of view (FOV):190 mm, image matrix: 64 * 64, slice thickness: 4 mm and number of axial slices:38) for total 100 volumes. During the rs-fMRI scans, the subjects were asked to close their eyes and "rest" (i.e., "doing nothing and keeping the mind wandering without particular thinking"). For the task fMRI scans, a boxcar paradigm with five on-off acquisitions as a period and ten periods was applied. The subjects were asked to perform a finger tapping task with the right hand (i. e., four fingers one by one touched the thumb in approximate 1 Hz frequency) in the "on" acquisitions, and to rest in the "off" acquisitions, and the task performance for each subject was guaranteed by watching his or her finger tapping and by displaying real-time BOLD fMRI signals during the fMRI scan.

2.3. Data processing

The rs-fMRI and the task fMRI data were analyzed offline in an individual and a group analyses for the patients and healthy subjects. For the individual analysis, AFNI (Cox, 1996) software was applied. First, the functional cortices (i.e., primary sensory and motor cortices and supplementary motor area (SMA)) were determined from the task fMRI data by a correlation coefficient analysis (i.e., a general linear method), and then the corresponding functional connectivity (FC) map for the sensory and motor network were determined from the rs-fMRI data by applying a seed method. The hand motor functional areas in both brain hemispheres of a subject were determined by the center of the cluster with at least five voxels which had the highest correlation co-efficiency values in the cortices, and the seed location was then placed in the center of the cluster in the right side cortices (i.e., the non-tumor side for the patients) determined by the task driven functional maps. The corresponding P value (uncorrelated) for the highest correlation value for each subject was different, and is from $5.2 * 10^{-29}$ to $3.4 * 10^{-14}$. By applying the seed method, the coordinates

Table 2
Healthy subjects.

No.	Sex/age
1	M/28
2	M/23
3	F/25
4	M/56
5	M/17
6	M/38
7	M/37
8	M/50
9	M/24
10	M/57

of the center for the cluster in each determined left side hand motor area in the network for each case were recorded. The coordinates of the hand motor voxel in the anatomical images were determined by the omega shape read by two experienced co-authors in neuro-radiology and neuro-surgery. Finally, the distances for the left side hand motor areas in the primary sensory and motor cortices (i.e., the tumor side for the patients) determined from the task fMRI data to the ones determined from the rs-fMRI data and the anatomical images were calculated from the coordinates. The maximum and mean values of the distances with the standard deviations for the 25 patients and 10 healthy cases were evaluated.

For the group analyses, both AFNI and FSL (Smith et al., 2004) software were applied for the data of the rs-fMRI and task fMRI groups for the patients and the healthy subjects. First the data of rs-fMRI and task fMRI for each case were run in AFNI for a motion and baseline corrections. The rs-fMRI data were then filtered for only keeping the frequencies in the band of 0.01 to 0.08 Hz since only these frequencies might result from neuronal functional connectivity (Leopold et al., 2003). Separately, the task fMRI data then were spatial smoothed by a 4 mm Gaussian function. After these steps, a multi-session temporal concatenation independent component analysis (ICA) was applied in FSL for determining the sensory and motor networks of the 25 patients and the 10 healthy subjects for the rs-fMRI group; and a multi-session tensor independent component analysis (ICA) was applied in FSL for determining the hand areas in the sensory and motor cortices of the patients and the healthy subjects for the task fMRI group. The coordinates of the pixels with the maximum correlation co-efficiencies either in the sensory and motor networks or in the sensory and motor cortices of the left side were recorded in AFNI. The distances for the groups were obtained from the calculation by using the coordinates.

3. Results

3.1. Patients

For these 25 patients, we applied the task fMRI and DTI data to determine the hand areas of sensory and motor cortices for generating presurgical plans, and successfully verified the hand areas in the tumor sides during the surgeries where indicated, by the gold standard: intra-operative electrical stimulation technique. The match of the hand areas to these areas suggested by the gold standard demonstrates that the hand areas determined by the task fMRI are accurate for such localization.

In Fig. 1, we show the hand areas by the green crosshairs on the tumor side (i.e., the left hemisphere) determined from the anatomical images (A), and the maps generated from the task (i.e., right hand finger

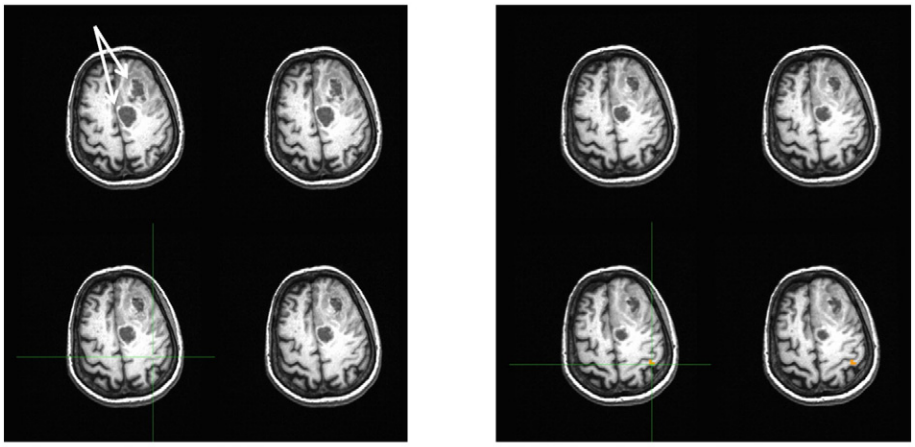

(1A) (1B)

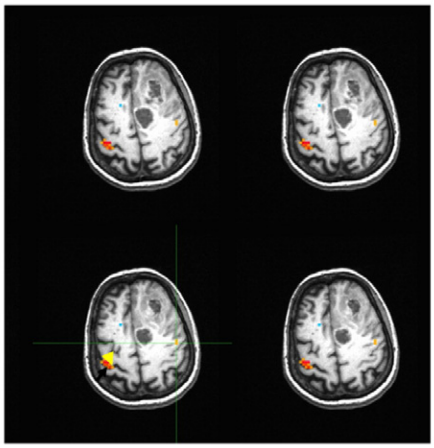

(1C)

Fig. 1. The hand area shown by the green crossheads determined by the anatomical images (1 A) and the maps generated from the task fMRI (1B) and rs-fMRI (1C) data for the 3rd case in Table 1. The yellow and black arrows point to the "seed" area and the two white arrows point to the tumors. For the maps, the left side is the right side.

tapping) fMRI (B), and rs-fMRI (C) Images for patient number three with an astrocytoma shown by two white arrows. For this case, the hand voxel is in the middle of the pre-central sulcus (i.e., the middle of the omega shape), at the middle of the pre-central gyrus, and at the far left pre-central gyrus determined respectively by the anatomical images, the task fMRI and rs-fMRI maps.

The coordinates of the hand areas in the left side sensory and motor cortices determined from the task fMRI or evaluated from the anatomical T1 images or in the left sensory-motor network resulted from the rs-fMRI data for the patients were recorded, and the distances (mm) between the three hand areas were calculated from the coordinates of the areas for each patient were listed in Table 3.

The 1st distance is between the hand areas determined by the task fMRI and rs-fMRI data, it varies from 2.57 to 44.30 mm (the 1st column in Table 3), and the average distance with standard deviation is 18.9 ± 10.61 mm. The 2nd distance is between the hand areas determined by the task fMRI and anatomic images, it varies from 5.13 to 36.52 mm (the 2nd column in Table 3), and the average distance with standard deviation is 21.37 ± 8.98 mm. The 3rd distance is the one between the hand areas determined by the rs-fMRI and anatomic images, it varies from 4.06 to 59.75 mm (the 3nd column in Table 3), and the average distance with standard deviation is 26.76 ± 15.14 mm.

The 3-dimensional (3D) locations (mm) of the hand areas for the 25 cases are plotted in Fig. 2. The hand areas determined by the task fMRI data (the stars) are distributed close to each other, however, the areas determined anatomically (the squares) and by the rs-fMRI data (the cycles) are distributed further apart, especially along the x direction. For many cases, the spatial locations of the areas determined by the task fMRI data are obviously different when they are compared to the areas determined by the rs-fMRI data or anatomical images.

For a better or fairer comparison on the locations of the hand areas of the left side determined by the task and the rs-fMRI, we performed group analyses on the data of the task and the rs-fMRI. For performing pre-surgical planning, we only used the results from the individual analyses. The group analyses are included in this paper for discussing the locations or "fingerprints" of the hand areas in the sensory and motor cortices of the left side for the patients.

We generated group 2D and 3D hand functional area maps and FC maps of the sensory-motor cortex of the tumor patients, shown in Fig. 3 in which Fig. 3A shows the hand functional area maps from the task fMRI data and Fig. 3B shows the FC maps from the rs-fMRI data. The maps demonstrating FC of the sensory and motor network are bilateral and almost symmetrical for the two hemispheres. As a comparison, the motor fMRI maps showed a left-lateralized pattern for the right hand finger task. In addition the supplementary motor area (SMA) was only detected in the FC maps.

Based on the tumor group images, we measured the coordinates of the hand area in the left side (i.e., the tumor side) determined from the task fMRI and rs-fMRI data for the group of the 25 patients with the brain tumors in the left side. The distance (mm) between the two hand areas determined by the coordinates of the task fMRI and the rs-fMRI data is 9.17 mm.

Table 3
The distances (mm) between the hand areas on the left side calculated from the coordinates (mm) of the task fMRI and rs-fMRI data and the anatomic images for the 25 patients.

No.	Distance (mm) between the hand areas determined by the finger tapping fMRI and the rs-fMRI data	Distance (mm) between the hand areas determined by the finger tapping fMRI data and the anatomical images	Distance (mm) between the hand areas determined by the rs-fMRI data and the anatomical images
1	10.28	7.49	6.93
2	25.32	18.28	38.06
3	27.20	25.46	9.95
4	11.90	16.67	23.69
5	35.15	35.31	59.75
6	24.19	10.81	21.86
7	6.70	36.52	37.95
8	44.30	29.75	32.16
9	6.51	5.13	11.59
10	9.89	32.59	40.88
11	20.52	19.70	4.06
10	19.82	17.65	24.57
13	9.48	23.05	14.69
14	2.57	13.88	13.01
15	25.78	17.94	30.58
16	11.13	20.25	21.82
17	10.73	20.05	13.97
18	30.53	33.74	51.72
19	13.69	28.48	21.42
20	26.76	29.09	49.47
21	29.14	14.46	35.52
22	15.76	11.75	25.03
23	20.80	21.44	5.02
24	23.70	12.70	19.86
25	24.05	29.37	49.55

3.2. Healthy subjects.

For the No. 7 in Table 2, the hand areas in the sensory and motor cortices of the left side are indicated by the green crosshairs in Fig. 4. The areas were determined by the anatomical images (4 A) and the maps generated from the task (i.e., the right hand finger tapping) fMRI (4B) and rs-fMRI (4C, the yellow arrow points to the "seed" area) data for this subject. For this case, the hand voxel is at the middle of the pre-central sulcus (i.e., the middle of the omega shape), at the left of the pre-central sulcus, and at the left post-central sulcus determined respectively by the anatomical images, the task fMRI and rs-fMRI maps.

The coordinates of the hand functional areas in the left side sensory and motor cortices were determined and recorded from the task fMRI and rs-fMRI data and the anatomical images for the 10 healthy subjects, and the distances (mm) between the three hand areas determined by the coordinates of the areas for each subject in the 10 cases are listed in Table 4.

The 1st distance is between the hand areas determined by the coordinates of the areas of the task fMRI and rs-fMRI. It varies from 2.28 to 18.97 mm (the first column in Table 4), and the average distance with standard deviation is 11.3 ± 5.41 mm. None of these distances is longer than 20 mm. The 2nd distance calculated is between the hand areas of the task fMRI and anatomic images, it varies from 5.45 to 20.40 mm (the 2nd column in Table 4), and the average distance with standard deviation is 10.46 ± 4.75 mm. Only one of the distances is longer than 20 mm. The 3rd distance is between the hand areas of the resting state fMRI and anatomic images, it varies from 7.88 to 40.51 mm (the 3nd column in Table 4), and the average distance with standard deviation is 23.13 ± 11.44 mm. Six of the distances (i.e., 60%) are longer than 20 mm.

The 3D locations of the hand areas for the 10 subjects are plotted in Fig. 5. The hand areas determined by the anatomical images, and the task and the resting state fMRI data are all close to each other for all cases.

We also made group 2D and 3D fMRI and FC maps for the10 subjects in Fig. 6 in which the left is the sensory and motor fMRI maps from the task fMRI data, and the right is the FC maps of the sensory and motor network from the rs-fMRI data. The maps show that, both the FC maps for the sensory and motor network and the sensory and motor functional maps are bilateral and almost symmetrical for the two hemispheres. The supplementary motor area (SMA) was also only detected in the sensory and motor network (i.e., the FC) maps.

We also measured the coordinates of the hand areas for the left side sensory and motor cortices determined from the task fMRI and the sensory and motor networks from the rs-fMRI group data for the group with 10 healthy subjects. The distance (mm) between the two hand areas determined by the task fMRI and the rs-fMRI group data based on the coordinates is 10.04 mm.

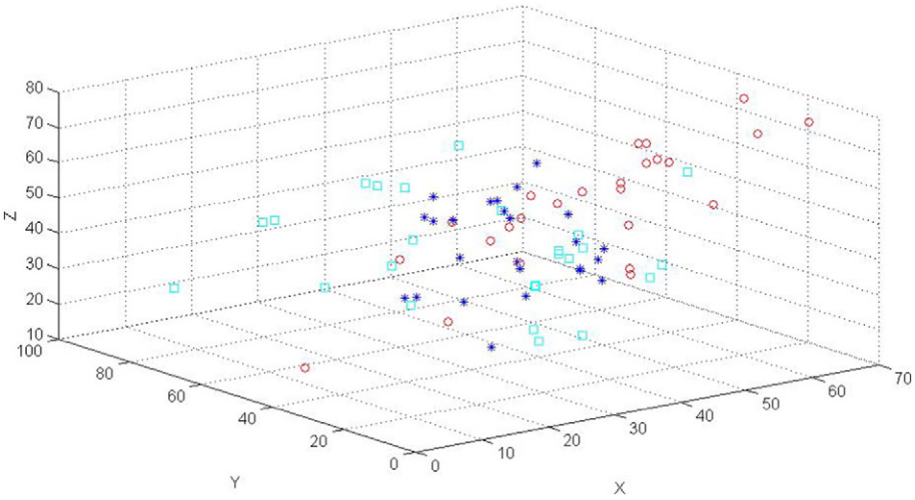

Fig. 2. A 3D plot (ftap (star), resting (cycle) and ana (square)) for the locations of the voxels of the hand areas in the sensory and motor cortices (or networks) of the tumor (i.e., the left) sides for the 25 cases.

4. Discussion

Clinically surgery for intrinsic brain lesions near the motor cortex remains challenging because of the risk of postoperative motor deficits. Preoperative imaging such as DTI can often show the relationship of the lesion to the putative motor tracts, but identification of the pyramidal tracts itself is dependent upon the precise localization of the motor strip. When the tumor is close to the motor strip anatomical landmarks are not well visualized and it may be unclear whether the lesion is behind the pyramidal tracts and is pushing them forwards or it is anterior to the tracts and pushing them backwards. This is important to differentiate because if the craniotomy is located anterior to the motor strip, and the motor tracts are being pushed forward by a lesion behind the motor tract; then surgery will not be possible without significantly harming the patient. Even intraoperative direct cortical stimulation and identification of the motor strip may not answer this question for certain

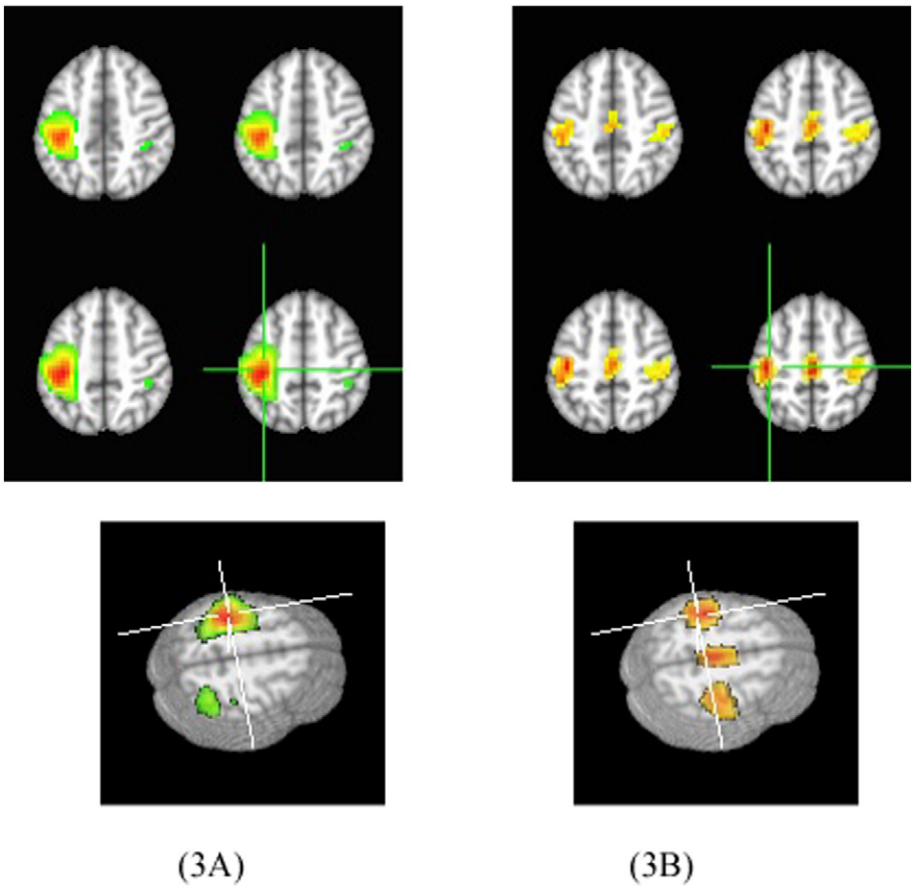

Fig. 3. The 2D and 3D maps for the tumor group with 25 cases, on the left are the sensory and motor functional maps generated by the right hand finger tapping fMRI data and on the right are the FC maps for the sensory and motor network generated by the rs-fMRI data. In the images, the left is the left side.

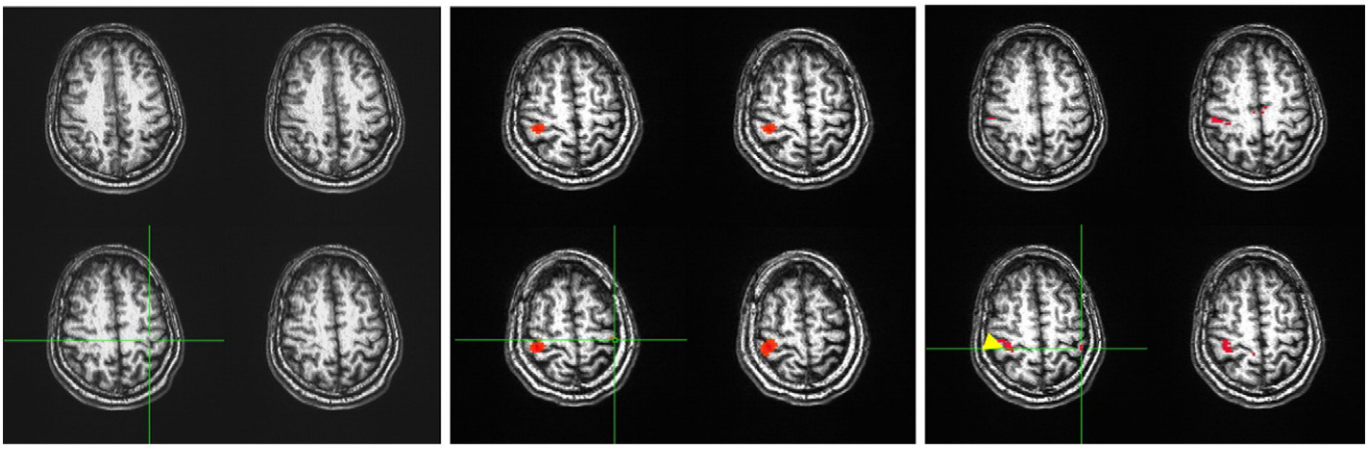

Fig. 4. The anatomical images (A) and the maps shown the hand areas in the sensory and motor cortices generated from the finger tapping task fMRI data (B), rs-fMRI (C) data for the 7th case in Table 2. The yellow arrow points to the "seed" area. The left side is the right side in the figure.

tumors. Therefore reliable identification of the motor strip preoperatively and thus identification of the pyramidal tracts and their relation to the tumor is necessary to plan a safe approach to the tumor. This identification is most often obtained from task driven BOLD fMRI data.

Tumors close to the motor cortex have a significant risk of postoperative hemiparesis or hemiplegia. The functional tissues (i.e., the areas) that need to be avoided for this study are the motor cortex and the corticospinal tracts (motor tracts) as surgical damage in these areas will produce a permanent deficit. Identification of the motor cortex aids surgery in two ways. First by identifying the motor cortex an appropriate craniotomy can be planned as the location of the tumor can be judged to be either in front of or behind the motor cortex. Secondly when diffusion tensor imaging and tractography is performed it is very helpful to know which part of the corona radiate actually carries the motor tracts and how those tracts are related to the tumor to be excised. This can only be done with some degree of confidence if the location of the motor cortex is known. Since edema surrounding the tumor often obscures the cortical anatomy and the underlying tracts, finding the location of the motor cortex becomes very important preoperatively. Usually the location of the motor cortex is indicated by task driven fMRI and this is verified intra-operatively by cortical stimulation. The motor tracts can then be identified by sub-cortical stimulation and the tumor resected to within a few millimeters of the motor tracts while avoiding injury to this critical area.

Table 4
The distances (mm) between the hand areas in the sensory and motor cortices or networks on the left side determined from the coordinates of the areas for the 10 healthy subjects.

No.	Distance (mm) between the hand areas determined by the finger tapping fMRI and the rs-fMRI data	Distance (mm) between the hand areas determined by the finger tapping fMRI data and the anatomical images	Distance (mm) between the hand areas determined by the rs-fMRI data and the anatomical images
1	17.94	17.00	8.98
2	2.28	9.03	7.88
3	18.97	5.45	23.78
4	7.42	10.93	40.51
5	14.25	6.71	10.37
6	10.39	11.32	19.62
7	6.10	15.21	23.32
8	8.59	10.57	31.90
9	9.63	15.96	35.18
10	15.44	20.40	29.82

The right hand finger tapping task fMRI data of these 25 patients were used to successfully determine the hand areas of the sensory and motor cortices on the tumor side, and these areas were further verified by intra-operative electrical stimulation technique, in cases where the tumor margin was very close to the motor cortex. In a paper from Muller (Muller et al., 1996) with a larger patient population, they found that in 46 recordings, there was 100% correlation between the motor fMRI and the intraoperative stimulation map within 20 mm, and 67% correlation within 10 mm. Based on the literature (Yousry et al., 1997; Naidich and Brightbill, 1996) and our experience, we consider a 20 mm differences on the locations of the hand areas determined by the task and the rs-fMRI data and anatomical images to be significant in preoperative planning and performing a correctly located craniotomy, to allow maximum resection of the tumor with a minimal risk of damage to the motor cortex or subcortical tracts. Hence, at present the location (i.e., "fingerprint") of the hand areas determined by the task fMRI should be considered as one of the standards among these three MR imaging methods for making a presurgical plan since the motor cortex location determined by the task fMRI is verifiable by the gold standard: intraoperative stimulation.

We have chosen a distance of two centimeters as being significant because of the known anatomy of the motor strip, whereby a difference of more than two centimeters is likely to place the proposed motor function outside the true motor strip. In addition when reliable identification with two centimeters accuracy for the motor cortex and the descending motor tracts is possible a small precisely targeted craniotomy can be placed, either in front of or behind the central sulcus, the cortical entry can be placed safely in front of or behind the sensorymotor area, the lesion will be evident prior to reaching the pyramidal tracts and finally subcortical stimulation of the tracts can guide safe resection of the lesion and reduce or eliminate the risk of post-operative morbidity.

The tumor group analyses on the task and rs-fMRI data show that the determined hand areas are very close, and the distance between two areas is only 9.17 mm. This difference in the location of hand areas should not be considered to be clinically significant for an optimum resection of a brain tumor. With this small difference, it seems that on the group analyses level the rs-fMRI can do a clinically useful job of determining the hand area and so that this information can be used for pre-surgical planning.

However, since resection of a brain tumor is performed on an individual patient, group analysis data is meaningless for pre-surgical planning. The individual analyses presented (Table 3) show that in only three cases (the cases of 1, 9 and 14), the difference in the hand area distances for the three MR imaging methods were <20 mm. For 13 of the

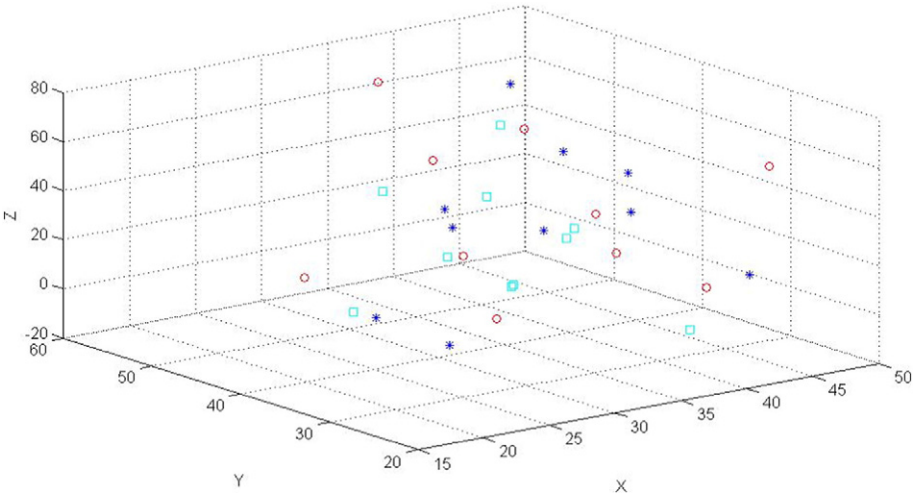

Fig. 5. A 3D plot (ftap (star), resting (circle) and ana (square)) for the locations of the voxels of the hand areas in the sensory and motor cortices (or networks) on the left sides for the 10 healthy subjects.

25 cases (52%) the distances between the task-determined hand areas and the rs-fMRI determined hand areas were >20 mm, and the average distance with standard deviation being 18.90 ± 10.61 mm. The obvious differences (i.e., the distances is longer than 20 mm) for the majority of cases suggests that the rs-fMRI data should not be the sole modality used for pre-surgical planning. A recent investigation (Rosazza et al., 2014) applying rs-fMRI and task fMRI on patients with lesions close to the sensorimotor cortex demonstrated that for 4 of the 13 cases (31%) the distance between the task-determined hand areas and the rs-fMRI determined hand areas were >20 mm. The authors of the study suggested rs-fMRI should not be considered as a replacement for task fMRI since localization performed by rs-fMRI is not equivalent to task fMRI (Rosazza et al., 2014).

Since we assume that the standard for determining the hand area fingerprint is from task driven (i.e. here right hand finger tapping) BOLD fMRI, we should also not rely on the use of anatomical information for determining the hand areas in the sensory and motor cortices since in 13 of 25 cases (52%) the distances were longer than 20 mm between the task-determined and the anatomically determined hand areas. The average distance was 21.37 ± 8.98 mm. Thus, the hand area should be determined at present only by the task BOLD fMRI signal. We believe that the location (i.e., the "fingerprint") of the hand area determined

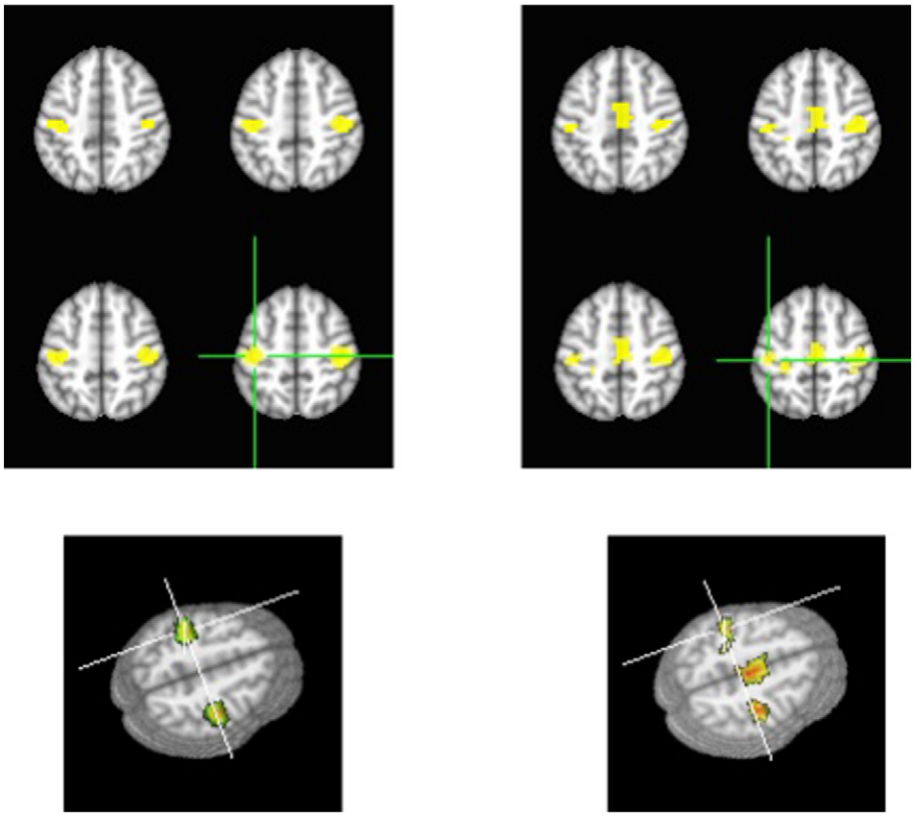

Fig. 6. The 2D and 3D maps for the healthy group with 10 cases. On the left are the motor functional maps generated by the right hand finger tapping fMRI data and on the right are the FC maps for the sensory and motor network generated by the rs-fMRI data. In the images, the left is the left.

by the task fMRI should be considered as the "gold" standard among the MR imaging methods.

The locations of the hand areas determined by the rs-fMRI and anatomical images were also differed in this study. The average distance with standard deviation was 26.76 ± 15.14 mm and in 16 of 25 cases (64%) the distance between these areas were >20 mm. The results of the hand area fingerprints in patients with brain tumors (see Table 3 and Fig. 2) by the three imaging methods clearly demonstrate there are three hand areas (i.e., three "fingerprints") in the sensory and motor cortices for every tumor case. The distances of the determined hand areas can be as small as a 2.57 mm to a significant 59.75 mm value.

Our study shows that while group rs-fMRI data tend to agree with the task fMRI as to the location of the hand motor functional areas of the patient group, individual analysis show wide variations in the rs-MRI data, rendering this modality unsafe for pre-operative planning for individual patients. Our experience with direct cortical stimulation has shown that the hand motor functional area is well localized by task based fMRI, as has been shown by others (Bizzi et al., 2008). A recent study (Mannfolk et al., 2011) has shown that rs-MRI and the task based fMRI were equally good in localizing the motor strip but this has not been our experience.

For the healthy subjects, the group analyses on the task and rs-fMRI data show that the distance between the determined hand areas was 10.04 mm. The individual analyses revealed that the distances between the hand areas determined by the task fMRI, rs-fMRI and anatomical images were in a range of 2.28 mm to 40.51 mm. The results from the group and individual analyses seem to suggest there are much smaller differences in the locations of the hand areas determined by these three imaging methods for healthy subjects as compared to patients harboring brain tumors. For example, in none of these 10 healthy subjects is the distance determined by the task and the rs-fMRI is >20 mm. Even for healthy subjects, the hand motor area is probably best indicated by task driven fMRI. The distance values from Table 4 suggest that the hand area locations determined from the task and rs-fMRI methods and from the task and anatomic imaging methods for each subject are fairly close. However, the distances determined from the rs-fMRI and anatomical images for six cases (i.e., 60%) are longer than 20 mm.

The different locations or fingerprints for the hand areas in the sensory and motor cortices determined by these three methods may be related to the assumptions underlying the mechanisms used to determine the location of the hand area by the different methods and tumor influences on the underlying mechanisms.

For applying anatomical imaging to determine a hand motor functional area, we sought the following signs or landmarks in a high resolution (a 0.9 mm isotropic voxel in this paper) T1 weighted images: the middle section of the omega or the sigmoidal hook sign with supplementary landmarks of superior frontal sulcus pre CS sign, pars bracket sign, Bifid post-CS sign, thin postcentral gyrus sign, intraparietal sulcus - post-CS, and midline sulcus sign (Naidich and Brightbill, 1996). Thus this area was determined by the imaging appearance and anatomical knowledge. However, a tumor close to the hand area may change the imaging appearance by changing T1, T2 and proton values. The local anatomy may be obscured by edema or mass effect and it may not be possible to recognize the hand area. Also in some patients, the hand functional area may be relocated to another adjacent brain area due to brain functional reorganization (Mathews et al., 2001; Hou et al., 2006a, 2006b; Shinoura et al., 2006). Hence, determination of hand areas for patients with brain tumors by anatomical images alone is not always sufficient or reliable.

For applying the rs-fMRI to determine the hand area in sensory and motor cortices, we rely on the functional connectivity of sensory and motor network which is determined by the intrinsic low-frequency fluctuations in the resting state BOLD fMRI signal. The signal is thought to reflect coherent neuronal activity in at least seven brain functional connected networks included this sensory and motor network, as demonstrated by studies combining electrophysiological recordings and rs-fMRI (Jann et al., 2010; Laufs et al., 2003; Mantini et al., 2007). The resting-state activity is considered to arise from the engagement of the brain networks necessary for performing tasks and/or responding to external stimuli such as performing a finger tapping and or a picture naming task (Mannfolk et al., 2011; Smith et al., 2009). Hence, the locations of the sensory and motor network may match primary sensory and motor cortices, however the hand area in the network based on the resting state BOLD fMRI signal can still be uncertain. In addition: the low frequency fluctuations in the resting-state BOLD signal is weak and usually mixed with other signal sources which are not related to neuronal functional activity even after a low frequency filter is applied (Davey et al., 2013).

In our study, we applied a seed method for the resting state signal to determine the locations of the hand areas on the side of the tumor (i.e., the left side). The seed method enhances the capacity to find the connected brain areas for a certain brain function if the seed area can be correctly selected and the whole resting state signal including the one in the seed area is only related to neuronal active BOLD signal. By using the task determined seed (i.e., the hand functional area) location in the non-tumor side; we then obtained the seed signal in the resting state BOLD fMRI signal for the location. Thus we were able to determine the hand area location, i.e., the hand fingerprint, on the tumor side by using the seed signal to perform a correlation analyses. Using the seed method, we have to assume that the influence from the tumor itself can be ignored for the resting state signal on the side of the tumor. This assumption may be questionable. This is if there are tumor effects in a tumor resting state BOLD fMRI data, the seed method for the hand area fingerprint can be mislabeled. We did not use the model independent methods such as independent component analysis because the resting data could not generate a stable or robust sensory and motor network for each individual in the patient group. The main reason for the lack of a robust sensory and motor network likely results from the tumor effects on the modification of the resting state signal.

For the task BOLD fMRI, we know that the signal is mainly related to CBF. The CBF increases in areas, due to response to a task such as a finger tapping, which correlates to the areas of neuronal functional activation if such areas do not include veins and arteries. The basis of applying BOLD mechanism for determining functional areas in eloquent cortices by task fMRI is that the neuronal functional activity and the change of CBF are tightly coupled for performing the task (Buxton et al., 2004). The task-driven BOLD fMRI signal is correlated to CBF, CBV and CMRO2 and the signal can be generated from the three parameters based on a balloon model (Buxton et al., 2004). For a patient with a GBM, the signal may not be detected due to the decoupling of the neovasculatures and neurons (Hou et al., 2006a, 2006b; Holodny et al., 1999). In this study with only one high grade gliomas (the case #13) in the frontal lobe which was also far to the primary sensory and motor cortices, since we accurately determined the hand area locations for the 25 patients by the task BOLD fMRI data we can say that there was such coupling between the neovasculature and the neurons in the hand functional areas, i.e., the neurons in the areas were responsible to the finger tapping stimulation of the patients.

However we do not know for certain how the rs-fMRI signal is related to neuronal functional activation areas which are determined by the task fMRI signal. It is unclear if the correlations among CBF, CBV and CMRO2 will still hold for the rs-fMRI signal. There are few publications (Zou et al., 2009; Wu et al., 2009; Chang et al., 2013; Mennes et al., 2010; Murphy et al., 2013) which suggest some underlying mechanisms. For the resting state fMRI signal, most people accept it to be the low frequency fluctuation of BOLD resulting from the synchronous neural activity. "However, despite the broad use of resting-state fMRI as a technique to investigate low-frequency BOLD fluctuations, the mechanisms that give rise to synchronous, spontaneous neural activity across brain regions remain largely unknown (Leopold and Maier, 2010)". Hence, the resting state BOLD signal may show functionally connected

areas including the sensory and motor network, but this does not mean the hand area location in the sensory and motor network can be accurately determined by the signal, even if the location of the sensory and motor network can be the same as the sensory and motor cortex determined by the task BOLD fMRI signal.

Considering the voxel size of the rs-fMRI and the task fMRI as approximate 3 mm^3, we demonstrate in this study that for the majority of the tumor cases the distances of the hand motor functional areas determined from the three MRI methods are longer than 20 (± 3) mm and the areas determined from the task fMRI were accurate in the localization of the motor cortex when intra-operative stimulation was performed on selected cases.

In future, as we accumulate more patients we will be able to generate enough data to separate low grade gliomas, high grade gliomas and other lesions such as cavernomas and AVM's to address the role of neurovascular de-coupling and its impact on BOLD MR imaging.

We will seek clinical correlates between distances and tumor grades to understand the effect of brain tumor on functional organization in ipsilateral hemisphere. Also we intent to show the correlate between the surgical outcome and the corresponding distance values to deliver the quantitatively clinical message to the pre-surgical planning of a patient with brain tumor.

For the hand functional areas determining by rs-fMRI, we will apply a new method: time-varying resting-state functional connectivity (Keilholz, 2014) for a farther justification on our main findings and novelty.

In a word, we would like to turn the clinical practice of qualitative fMRI to a quantitative method (i.e., to have the fingerprint of every functional area for each brain tumor patient) for optimization of brain tumor resection.

5. Conclusions

1) For majority of the 25 tumor cases, the locations of the hand motor area in the tumor sides determined from an rs-fMRI data and anatomical images are more than 20 mm apart from the one determined from a finger tapping fMRI data. None of 10 healthy subjects the distance of the locations of the hand motor areas determined from rs-fMRI and the task fMRI is longer than 20 mm.

2) The differences in the locations or fingerprints of the hand motor areas determined by these three MR methods for the patients result from differences in mechanisms of the three modalities for determining the localization and tumor effects on the mechanisms: 1) task driven (finger tapping) BOLD fMRI signal is for determining active neurons in the sensory and motor cortices; 2) resting state BOLD fMRI signal is for determining "neuronal' functional connectivity in the sensory and motor network; and 3) anatomical landmarks in a high resolution T1 images are applied for locating the hand motor area in the sensory and motor cortices.

3) At present for performing pre-surgical planning, as long as there is a coupling between neuronal activation and neurovasculatory the task fMRI is accurate for localizing the hand motor functional areas of the patients. rs-fMRI as performed, is not a suitable replacement for the task fMRI in performing the pre-surgical planning of a patient with brain tumor.

Acknowledgements

The authors acknowledge the financial support from NIH COBRE grant (Neuroscience Grant GM103503), and the important support in the organization by Dr. C. Rosen (the chairman of the Department of Neurosurgery, WVU) and by Dr. M. Frick (the chairman of the Department of Radiology, WVU).

References

Alkhadi, H., Kollias, S.S., Crelier, G.R., et al., 2000. Plasticity of the human motor cortex in patients with arteriovenous malformations: a functional MR imaging study. Am. J. Neuroradiol. 21, 1423–1433.
Biswal, B.B., Yetkin, F.Z., Haughton, V.M., et al., 1995. Functional connectivity in the motor cortex of resting human brain using echo-planar MRI. Magn. Reson. Med. 34, 537–541.
Biswal, B.B., Mennes, M., Zuo, X.N., et al., 2010. Toward discovery science of human brain function. Proc. Natl. Acad. Sci. U. S. A. 107 (10), 4734–4739.
Bizzi, A., Blasi, V., Falini, A., et al., 2008. Presurgical functional MR imaging of language and motor functions: validation with intraoperative electrode mapping. Radiology 248, 579–589.
Buxton, R.B., Uludag, K., Dubowitz, D.J., et al., 2004. Modeling the hemodynamic response to brain activation. NeuroImage 23, S220–S233.
Carpentier, A.C., Constable, R.T., Schlosser, M.J., et al., 2001. Patterns of functional magnetic resonance imaging activation in association with structural lesions in the rolandic region: a classification system. J. Neurosurg. 94, 946–954.
Chang, C., Liu, Z., Chen, M.C., et al., 2013. EEG correlates of time-varying BOLD functional connectivity. NeuroImage 72, 227–236.
Cordes, D., Haughton, V.M., Arfanakis, K., et al., 2000. Mapping functionally related regions of brain with functional connectivity MR imaging. AJNR Am J Neuroradiol 21, 1636–1644.
Cordes, D., Haughton, V.M., Arafanakis, K., et al., 2001. Frequencies contributing to functional connectivity in the cerebral cortex in 'resting state' data. AJNR Am. J. Neuroradiol. 25, 1326–1333.
Cox, R.W., 1996. AFNI: software for analysis and visualization of functional magnetic resonance neuroimages. Comput. Biomed. Res. 29 (3), 162–173.
Davey, C.E., Grayden, D.B., Egan, G.F., et al., 2013. Filtering induces correlation in fMRI resting state data. NeuroImage 64, 728–740.
De Luca, M., Smith, S.M., De Stefano, N., et al., 2005. Blood oxygenation level dependent contrast resting state networks are relevant to functional activity in the neocortical sensorimotor system. Exp. Brain Res. 167, 587–594.
Deshpande, G., Santhanam, P., Hu, X., 2011. Instantaneous and causal connectivity in resting state brain networks derived from functional MRI data. NeuroImage 54 (2), 1043–1052.
Duffau, H., 2001. Acute functional reorganization of the human motor cortex during resection of central lesions: a study using intraoperative brain mapping. J. Neurol. Neurosurg. Psychiatry 70, 506–513.
Emerson, R.G., Turner, C.A., 1993. Monitoring during supratentorial surgery. J. Clin. Neurophysiol. 10 (4), 404–411.
Fandino, J., Kollias, S.S., Wieser, H.G., et al., 1999. Intraoperative validation of functional magnetic resonance imaging and cortical reorganization patterns in patients with brain tumors involving the primary cortex. J. Neurosurg. 91, 238–250.
Fiecas, M., Ombao, H., van Lunen, D., et al., 2013. Quantifying temporal correlations: a test-retest evaluation of functional connectivity in resting-state fMRI. NeuroImage 65, 231–241.
Foz, M.D., Raichle, M.E., 2007. Spontaneous fluctuations in brain activity observed with functional magnetic resonance imaging. Nat. Rev. Neurosci. 8, 700–711.
Holodny, A.I., Schulder, M., Liu, W.C., et al., 1999. Decreased BOLD functional MR activation of the motor and sensory cortices adjacent to a glioblastoma multiforme: implications for image-guided neurosurgery. AJNR Am J Neuroradiol 20, 609–610.
Hou, B.L., Holodny, A.I., Cooperman, N., et al., 2006a. Reorganization of the cortical control of movement due to radiation necrosis. Case report. J Neurosurg 104 (1), 147–149.
Hou, B.L., Bradbury, M., Peck, K.K., et al., 2006b. Effect of brain tumor neovasculature defined by rCBV on BOLD fMRI activation volume in the primary motor cortex. NeuroImage 32 (2), 489–497.
Jann, K., Kottlow, M., Dierks, T., et al., 2010. Topographic electrophysiological signatures of fMRI resting state networks. PLoS One 5 (9), e10945.
Keilholz, S.D., 2014. The neural basis of time-varying resting-state functional connectivity. Brain connectivity 4 (10), 769–779.
Kokkonen, S.M., Nikkinen, J., Remes, J., et al., 2009. Preoperative localization of the sensorimotor area using independent component analysis of resting-state fMRI. Magn. Reson. Imaging 27, 733–740.
Laufs, H., Krakow, K., Sterzer, P., et al., 2003. Electroencephalographic signatures of attentional and cognitive default modes in spontaneous brain activity fluctuations at rest. Proc. Natl. Acad. Sci. U. S. A. 100, 11053–11058.
Lehericy, S., Duffau, H., Cornu, P., et al., 2000. Correspondence between functional magnetic resonance imaging and somatotropy and individual brain anatomy of the central region: comparison with intraoperative stimulation in patients with brain tumors. J. Neurosurg. 92, 589–598.
Leopold, D.A., Maier, A., 2010. Ongoing physiological processes in the cerebral cortex. NeuroImage 62, 2190–2500.
Leopold, D.A., Murayama, Y., Logothetis, N.K., 2003. Very slow activity fluctuations in monkey visual cortex: implications for functional brain imaging. Cereb. Cortex 13, 425–433.
Liu, H., Buckner, R.L., Talukdar, T., et al., 2009. Task-free presurgical mapping using functional magnetic resonance imaging intrinsic activity. J. Neurosurg. 111, 746–754.
Long, X.Y., Zuo, X.N., Kiviniemi, V., et al., 2008. Default mode network as revealed with multiple methods for resting-state functional MRI analysis. J. Neurosci. Methods 171 (2), 349–355.
Lowe, M.J., Mock, B.J., Sorenson, J.A., 2001. Functional connectivity in single and multislice echoplanar imaging using resting state fluctuations. NeuroImage 7, 119–232.
Majos, A., Tybor, K., Stefanczyk, L., et al., 2005. Cortical mapping by functional magnetic resonance imaging in patients with brain tumors. Eur. Radiol. 15, 1148–1158.
Mannfolk, P., Nilsson, M., Hansson, H., et al., 2011. Can resting-state functional MRI serve as a complement to task-based mapping of sensorimotor function? A test–retest reliability study in healthy volunteers. J. Magn. Reson. Imaging 34, 511–517.

Mantini, D., Perrucci, M.G., Del Gratta, C., et al., 2007. Electrophysiological signatures of resting state networks in the human brain. Proc. Natl. Acad. Sci. U. S. A. 104, 13170–13175.
Mathews, S., Oommen, K.J., Francel, P., 2001. Functional reorganization of motor cortex due to brain tumor: a case report. J Okla State Med Assoc 94 (1), 7–11.
Mennes, M., Kelly, C., Zuo, X.N., et al., 2010. Inter-individual differences in resting-state functional connectivity predict task-induced BOLD activity. NeuroImage 50 (4), 1690–1701.
Mesulam, M.M., 2000. Principles of Behavioral and Cognitive Neurology. Oxford University Press, Oxford, pp. 102–140.
Muller, V.M., Yetkin, F.Z., Hammeke, T.A., et al., 1996. Functional magnetic resonance mapping of the motor cortex in patients with cerebral tumors. Neurosurgery 39, 515–520.
Murphy, K., Birn, R.M., Bandettini, P.A., 2013. Resting-state fMRI confounds and cleanup. NeuroImage 80, 349–359.
Naidich, T.P., Brightbill, T.C., 1996. Systems for localizing fronto-parietal gyri and sulci on axial CT and MRI. Int. J. Neuroradiol. 2, 313–338.
Otten, M.L., Mikell, C.B., Youngerman, B.E., et al., 2009. Motor deficits correlate with resting state motor network connectivity in patients with brain tumours. Brain 135 (Pt4), 1017–1026.
Raichle, M.E., MacLeod, A.M., Snyder, A.X., et al., 2001. A default mode of brain function. Proc. Natl. Acad. Sci. U. S. A. 16, 676–682.
Roessler, K., Donat, M., Lanzenberger, R., et al., 2005. Evaluation of preoperative high magnetic field motor functional MRI (3 Tesla) in glioma patients by navigated electrocortical stimulation and postoperative outcome. J. Neurol. Neurosurg. Psychiatry 76, 1152–1157.
Rosazza, C., Aquino, D., D'Incerti, L., Cordella, R., Andronache, A., Zaca`, D., et al., 2014. Preoperative mapping of the sensorimotor cortex: comparative assessment of task-based and resting-state fMRI. PLoS One 9 (6), 1–19.
Rutten, G.J., Ramsey, N.F., 2010. The role of functional magnetic resonance imaging in brain surgery. Neurosurg. Focus. 28, E4.
Shinoura, N., Suzuki, Y., Yamada, R., et al., 2006. Restored activation of primary motor area from motor reorganization and improved motor function after brain tumor resection. AJNR Am J Neuroradiol 27 (6), 1075–1082.
Smith, S.M., Jenkinson, M., Woolrich, M.W., et al., 2004. Advances in functional and structural MR image analysis and implementation as FSL. NeuroImage 23, S208–S219.
Smith, S.M., Fox, P.T., Miller, K.L., et al., 2009. Correspondence of the brain's functional architecture during activation and rest. Proc. Natl. Acad. Sci. U. S. A. 106 (31), 13040–13045.
Uddin, L.Q., Kelly, A.M., Biswal, B.B., et al., 2009. Functional connectivity of default mode network components: correlation, anticorrelation, and causality. Hum. Brain Mapp. 30 (2), 625–637.
Wu, C.W., Gu, H., Lu, H., et al., 2009. Mapping functional connectivity based on synchronized CMRO2 fluctuations during the resting state. NeuroImage 45 (3), 694–701.
Xiong, J., Parsons, L.M., Gao, J.H., et al., 1999. Interregional connectivity to primary motor cortex revealed using MRI resting state images. Hum. Brain Mapp. 8, 151–156.
Yousry, T.A., Schmid, U.D., Alkhadi, H., et al., 1997. Localization of the motor hand area to the knob on the precentral gyrus. a new landmark. Brain 100 (Pt 1), 141–157.
Zhang, D., Johnston, J.M., Fox, M.D., et al., 2009. Preoperative sensorimotor mapping in brain tumor patients using spontaneous fluctuations in neuronal activity imaged with functional magnetic resonance imaging: initial experience. Neurosurgery 65, S226–S236.
Zou, Q., Wu, C.W., Stein, E.A., et al., 2009. Static and dynamic characteristics of cerebral blood flow during the resting state. NeuroImage 48 (3), 515–524.
Zou, Q., Ross, T.J., Gu, H., et al., 2010. Intrinsic resting-state activity predicts working memory brain activation and behavioral performance. Hum. Brain Mapp. http://dx.doi.org/10.1002/hbm.25136.